International Journal of Engineering Research & Technology (IJERT)
ISSN: 2278-0181
Vol. 11 Issue 02, February-2022

Artificial Neural Network Modelling of the Tensile Characteristics of AISI 304l and 316l Stainless Steel Welded Joints at Ambient and Elevated Temperatures

M. A. R. R.R. Husain, S.S. Mohamed
Mechanical Engineering Department,
Faculty of Engineering at Shoubra,
Benha University, Cairo, Egypt.

***Abstract*:- In the current work, the AISI 316L and 304L austenitic stainless-steel (ASS) plates were joined to form similar and dissimilar welded joints. The gas tungsten arc welding (GTAW) was used to join the ASS plates. The filler material used for welding was ER308L filler rods. The welding voltage, welding current, and welding speed GTAW process parameters were kept constant at 38 V, 210 A, and 11 mm/sec., respectively. The microstructure and hardness of the welded joints were investigated. The temperature dependance of the tensile characteristics of the ASS welded joints, typically, the ultimate yield strength (YS), tensile strength (UTS) and elongation % (E%) were evaluated up to 300 ºC. Moreover, models based on Radial Basis Function (RBF) and Multi-Layer Perceptron (MLP) ANN techniques were developed to predict the tensile characteristics as function of the temperature and base material type. The results revealed that, at elevated temperatures, increasing the temperature reduces the UTS and YS, but increases ductility, of the investigated similar and dissimilar ASS welded joints. The generated ANN models can precisely predict the tensile characteristics of the similar and dissimilar AISI 304L and AISI 316L ASSs welded joints with a very high accuracy. The generated ANN models based on MLP and RBF techniques with layer structures of 2-5-3 and 2-9-3, respectively, exhibited the best performances for modelling the tensile properties of the welded joints. The mean absolute error (MAE) developed from the MLP and RGB models are about 7.69 and 7.45, respectively.**

Keywords: Austenitic Stainless Steels, Tungsten Inert Gas (TIG), Gas Tungsten Arc Welding, Tensile Properties, Artificial Neural Networks, Elevated Temperatures.

1. INTRODUCTION

Austenitic stainless steel (ASS) is the largest family of stainless-steel (SS) alloys. It occupies about 2/3 of all SS production. They have an austenitic microstructure, which is attained by alloying with sufficient Ni and/or Mn and N to keep an austenitic microstructure at all temperatures from the cryogenic region to the melting point [1]. Austenitic SS is not hardenable by heat treatment because they retain the same microstructure at all temperatures. However, it can be strengthened using other techniques such as cold working. The austenitic microstructure provides the ASS outstanding formability and weldability. The most widely used ASS grades are the 18/9 types (i.e., AISI 304 and 304L), which form more than 50% of the worldwide production of SS.

The GTAW process, known also as Tungsten inert gas (TIG) welding process is widely used for welding SS [2]. It has several advantages like narrow fusion zone (FZ), small size welding pool, excellent metallurgical quality of the weld, and oxidation residues are eliminated [3]. In GTAW, the energy needed for melting the metal is provided by an electric arc hit and kept between the electrode and the workpiece, under atmosphere of an inert gas. There are several shielding gases that can be used in GTAW, typically, argon (Ar), helium (He) and hydrogen (H_2) or a mixture of them. The inert gas shields the arc zone from the ambient air and keeps arc stability. If a filler metal is used, it is in the shape of either rods or coiled wire [4].

An artificial neural network (ANN) is a reproduction of the brain of a human. A natural brain can realize new things, fit to new and changing conditions. The brain exhibits the most amazing capability to analyze inadequate and uncertain, fuzzy information, and make its own judgment out of it [5]. The ANN consists of processing units known as neurons which tries to replicate the structure and behavior of the natural neuron. The ANN is used for data classification, pattern recognition, and in applications where data is unclear [6].

ANN was used for modelling and predicting the microstructural and mechanical characteristics of welded steel joints [7-11]. For example, *Bera* and *Das* [10], generated ANN model to estimate the mechanical properties of the weld dissimilar joint. The joint materials are 304L SS and EN8 mild steel plates and welded using gas metal arc welding (GMAW). The results revealed that quite close estimation of the ANN predicted values can be made with the observed tensile properties and the hardness of the welded joints. Also, *Ates et al.* [11], develop a new method based on ANN to estimate the material features for GMAW processes. The model predicts the mechanical properties, such as tensile strength, impact strength, elongation percentage, and hardness. It is showed that some predicted values are showed high accuracy, in contrast, some others predicted values showed relatively higher errors. Therefore, this approach may be used to predict, the elongation percentage and yield strength when the shielding gases ratios are determined before welding.

International Journal of Engineering Research & Technology (IJERT)
ISSN: 2278-0181
Vol. 11 Issue 02, February-2022

There is a lack of investigations about the modelling of the mechanical characteristics of stainless-steel welded joints to predict their behavior. Also, the influence of the temperature on the mechanical properties of such alloys is not modelled in these investigations. Consequently, the present investigation aims to develop ANN models to predict the tensile properties of similar and dissimilar stainless steel welded joints as a function of the temperature.

2. EXPERIMENTAL PROCEDURES

The AISI 304L ASS has the following chemical compositions (wt.-%): 18.91% Cr, 10.65% Ni, 2.01% Mn, 0.028% C, 1.1% Si, 0.03% S, 0.04% P, and Fe is the balance. The AISI 316L ASS has the following chemical compositions (wt.-%): 17.54% Cr, 11.89% Ni, 2.05% Mn, 0.026% C, 2.25% Mo, 1.02% Si, 0.018% S, 0.045% P, and Fe is the balance. The ER308L filler rod having 2.4 mm diameter was used as a filler. The E308L filler material has the following chemical composition (wt.-%): 19.8% Cr, 9.8% Ni, 1.9% Mn, 0.02% C, 0.4% Si, 0.15% Cu, 0.05% N, and Fe is the balance. The AISI 304L and AISI 316L SS plates were cut to smaller plates having length, width and thickness of 600 mm, 60 mm, and 10 mm, respectively. Before welding, the plates prepared to have a single V-groove with an angle of 60^o as shown in Fig. 1.

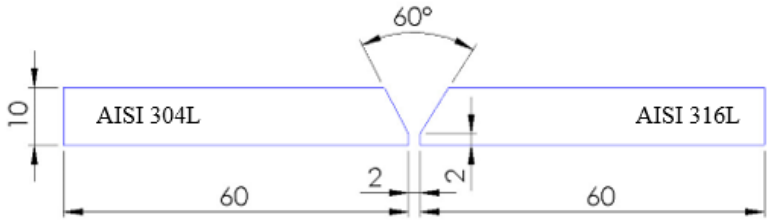

Figure 1. Typical dimensions (in mm) of the ASS joints.

The GTAW process was used to join similar ASS joints, like, AISI 316L to 306L and AISI 304L to 304L, and the dissimilar welded joints, like, AISI 304L to 316L. The GTAW process was carried out manually at constant welding voltage, welding current and welding speed of 38 V, 210 A, and 11 mm/sec, respectively. The GTAW process was performed using four passes.

After welding, the specimens for metallurgical investigations were cut and machined from the welded plates. The welded specimens were ground and polished the polishing/grinding machine. The welded specimens were ground using SiC emery papers with increasing finesses up to 1200 grit, followed by polishing using 0.1 µm alumina suspension on polishing clothes. Finally, the welded specimens were etched in an aqueous solution consists of 33% HNO_3 and 33% HCl acids for about 1 minute. The etching procedures were performed according to ASTM E407-07 [12]. The microstructural investigations of the welded joints were performed using optical metallurgical microscope.

The Vickers hardness (VHN) of the weld zone (WZ) was measured using a diamond pyramid indenter of a load of 100 kg for 10 s. The hardness profiles of the WZ were carried out on the cross-section perpendicular to the welding direction with a spacing of 1 mm. The VHN hardness measurements were carried out on welded specimens prepared for metallographic examinations.

Tensile tests of the similar and dissimilar welded joints were carried out at ambient, 100, 200 and 300 ^{o}C. The tensile tests were carried out using *Shimadzu* universal testing machine. The machine has a maximum load of 200 kN. Form each condition, approximately three specimens were tested. Figure 2 shows the dimensions of the tensile specimens. The smallest diameter of the specimen is at the center at which the welded region is located. Such design ensures that the fracture is taken place at the welded region.

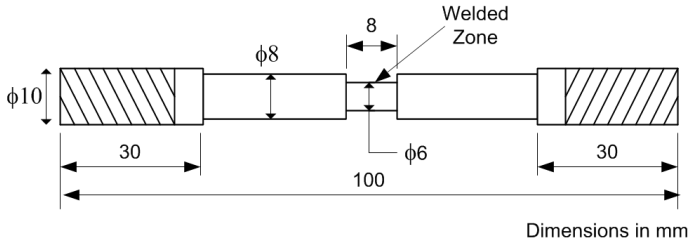

(a)

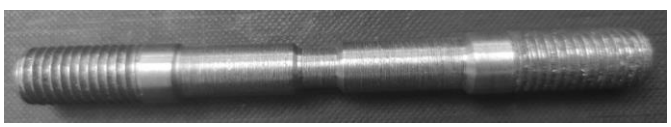

(b)

Figure 2. (a) dimensions of the tensile sample with the welded region at the center, (b) a photograph of typical welded tensile specimens.

International Journal of Engineering Research & Technology (IJERT)
ISSN: 2278-0181
Vol. 11 Issue 02, February-2022

The elevated temperatures were carried out using an electrical resistance furnace. Before testing, the tensile specimen was heated to the required temperature for at least 30 min to ensure that the temperature distribution inside the furnace is homogenous. The temperature inside the furnace was measured using a thermocouple. During the tensile tests, the crosshead speed was kept constant of 1 mm/min. Three replicates for tensile testing, for each condition, were prepared and the mean value of the ultimate tensile strength (UTS), yield strength (YS) and elongation (%) were determined.

The ANN technique is adopted for modeling the dependance of the tensile properties of the investigated similar and dissimilar ASS welded joints on both the temperature as well as the base material. The ANN models were constructed based on MLP and RBF approaches. The mean absolute error (MAE) was evaluated to determine the accuracy of the developed the models. The MAE estimates the average value of errors in a set of predictions, without taking into considerations their direction. The MAE can be estimated as follows [11]:

$$\mathrm{MAE} = \frac{\sum_{i=1}^{n} |y_i - x_i|}{n} = \frac{\sum_{i=1}^{n} |e_i|}{n} \quad \ldots(1)$$

The MAE is the mean of the absolute errors $|e_i| = |y_i - x_i|$, where y_i and x_i are the prediction and the experimental (true) values, respectively.

3. RESULTS AND DISCUSSION

3.1. Macro- and microstructural characteristics of the stainless-steel weldments

Visual observations of the 304L, 316L and 304L/316L welded joints showed that all joints were sound and free from defects. No macroscopic defects such as joint distortion, spatters …etc. were detected. However, examinations under optical microscope showed that some weld liquation microcracks at the roots of the 304L and 316L similar ASSs welded joints (see Fig. 3). Weld metal liquation cracking represents is specific to reheated weld metal (i.e., multi-pass welds). They are most often observed in single-phase weld metal of ASS and are always intergranular [1]. There was no observed evidence of microcracks or porosities in the 304L/316L ASSs dissimilar welded joints. The microstructure of the 304L and 316L ASS exhibited a typical equiaxed austenite grain structure. The microstructure of the 304L and 316L alloys contains uniform grain distribution containing two micro-constituents, typically, austenitic γ-phase (light) and the ferrite α-phase (dark).

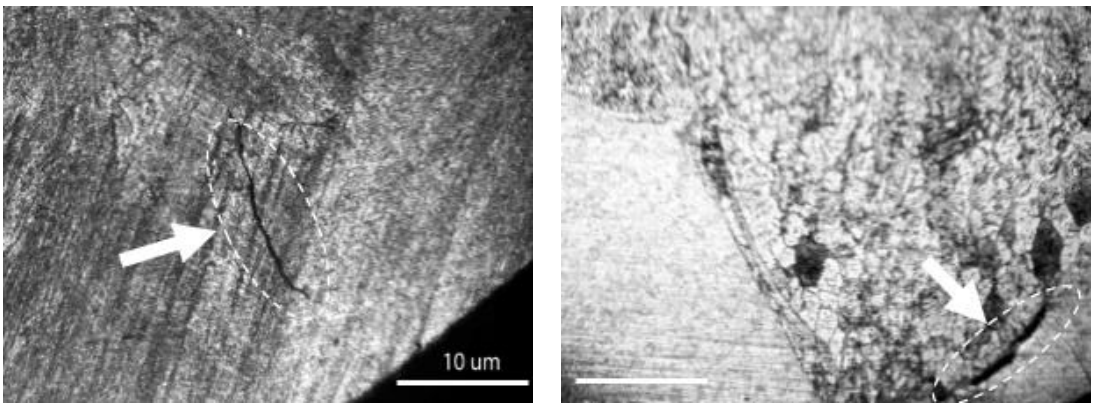

(a) (b)

Figure 3. The microcracks found in the roots of the (a) 304L and (b) 316L ASS welded joints.

Figures 4a and 4b shows the microstructure of the weld region (WR) of both 304L and 316L similar welded joints, respectively. The transition between the base metal and the weld metal is clearly seen. The results revealed that the size of the grains in heat affected zone (HAZ) are slightly larger than the base metal due to the heat input distribution. The growth of the grains found in the HAZ may be described with the assistance of thermal cycles taken place during GTAW process. The nearer to the fusion boundary, the higher the peak temperature and the longer period the material remains at higher temperatures. Since growth of the grains increases with increasing the temperature of annealing and time, the size of the grains in the HAZ increases as the fusion boundary is reached [13,14]. The weld metal shows needle like growth, and their growth is oriented in the direction of the center of the weld. However, the 304L weld metal exhibited larger grain size when compared with the 316L weld metal (compared Fig. 4a and 4b). Figures 4c and 4d show the microstructure of the 304L/316L dissimilar welded region. The figures show the welded regions at 304L and 316L sides, respectively. In the fusion zone (FZ) of both sides, the nearly equiaxed austenite grains with discontinuous network of pedate (γ)-ferrite structure in the austenitic matrix are clearly seen.

International Journal of Engineering Research & Technology (IJERT)
ISSN: 2278-0181
Vol. 11 Issue 02, February-2022

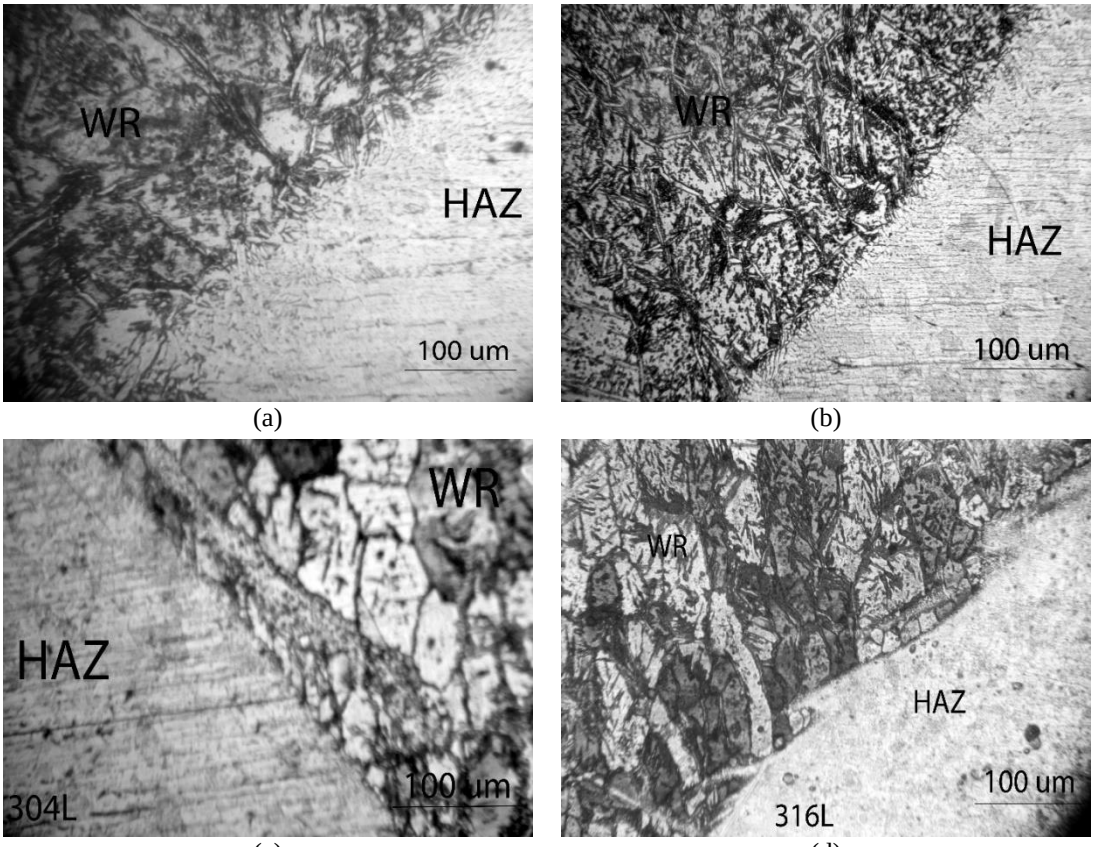

Figure 4. The microstructure of the 304L (a) and 316L (b) stainless steel similar welded regions; and the 304L/316L dissimilar welded region from the 304L (c) and 316L (d) sides.

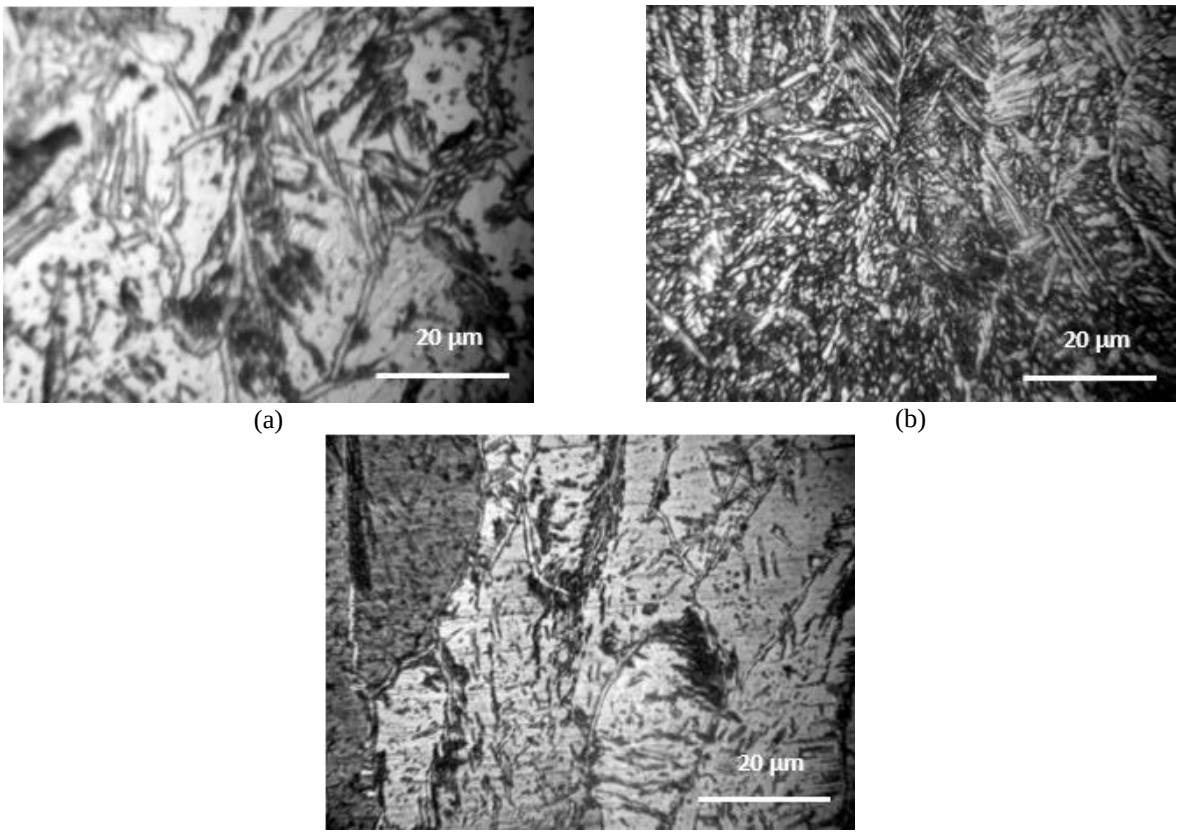

Figure 5. High magnification micrographs of the microstructure, at the center of the fusion zones, of (a) 304L, (b) 316L, and (c) 304L/316L ASS welded joints.

International Journal of Engineering Research & Technology (IJERT)
ISSN: 2278-0181
Vol. 11 Issue 02, February-2022

Figure 5 shows high magnification micrographs of the microstructure, at the center of the fusion zone, of 304L, 316L and 304L/316L ASSs welded joints. The FZs, welded by means of ER308L electrodes, exhibited microstructures that have a combination of lacy ferritic and acicular growth of ferrite in the austenitic matrix. It is clear from Fig. 5b that the amount of δ-ferrite content (dark) in the welded metal produced for 316L are much higher than for 304L and 304L/316L. This may attribute to the presence of molybdenum (Mo) in the 316L ASS [15]. It is well known that the Mo is an element that is sensitive to ferrite stabilizing [16].

3.2. Hardness of the stainless-steel welded joints

Figures 6 shows the hardness distribution at the weld regions for 304L, 316L and 316L/304L joints, respectively. The AISI 304L and AISI 316L ASS exhibited average hardness of 204±1 VHN and 203±2 VHN, respectively. In all cases, the FZ of the welded regions exhibited slightly higher hardness when compared with the base metal. The average hardness follows a decreasing trend in the order of weld metal, HAZ and base metal.

The center of the FZs of 304L, 316L and 316L/304L weld metal exhibited average hardness of 207±2 VHN, 207±3 VHN and 209±3 VHN, respectively. The increase of the hardness of the FZs when compared with the base metal may attribute to the variation of grains size at the welded region as well as the presence of the alloying elements found in the ER 308L filler rod which affect the ferrite structure in the metal weld region. The ER 308L filler rod has higher % of chromium (Cr) (19.8 wt.-%) when compared with the AISI 304L (18.91 wt.-%) and AISI 316L (17.54 wt.-%) ASSs which increases the hardness. In addition to the Cr %, the molybdenum (Mo) % also influences the hardness. The Cr and Mo elements increase Cr_{eq}/Ni_{eq} ratio and result in solidification phase with higher ferrite content.

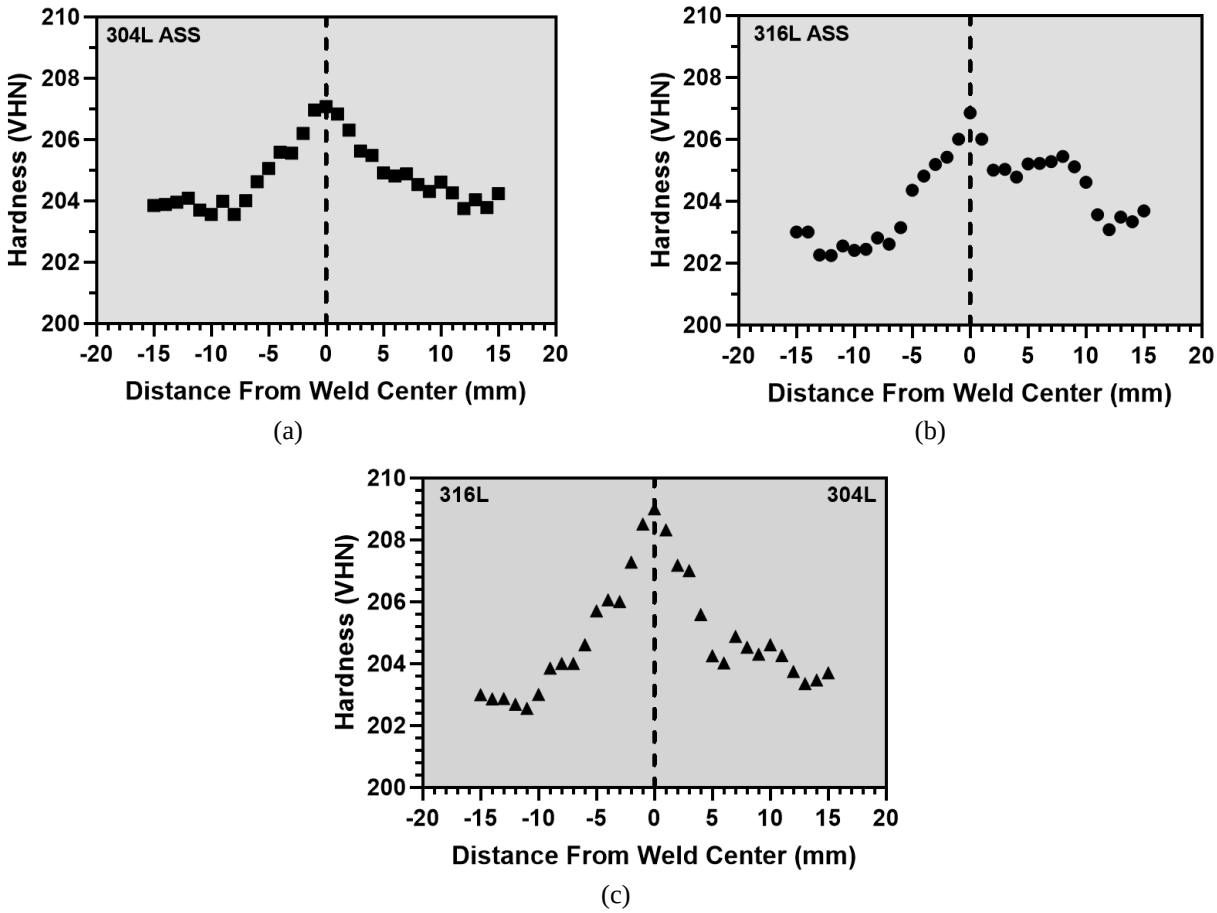

Figure 6. The hardness of the (a) 304L, (b) 316L, and (c) 316L/304L welded regions.

3.3. Tensile Characteristics of the ASS weldments at elevated temperatures

The ultimate tensile strength (UTS), at ambient temperature, of the 304L and 316L ASS base metals were found to be 498±5 MPa and 482±6 MPa, respectively. Figure 7a shows the variation of the UTS of the welded joints with temperature. At ambient temperature, the 304L welded samples showed higher average UTS (512±15 MPa) than the 304L base metal (498±5 MPa). Similarly, at ambient temperature, the 316L welded samples exhibited practically the same average UTS (480±10 MPa) of the 316L base metal (482±6 MPa). The dissimilar 304L/316L welded samples exhibited slightly lower UTS (467+10 MPa) than both 304L and 316L welded samples. Increasing the test temperature reduces the UTS of the welded joints. Such observation was

International Journal of Engineering Research & Technology (IJERT)
ISSN: 2278-0181
Vol. 11 Issue 02, February-2022

noticed for both similar and dissimilar 304L and 316L ASSs welded samples. For instance, increasing the test temperature of the AISI 304L-304L welded samples from ambient to 300 ºC, the average UTS was reduced from 512 MPa to 484 MPa. While for 304L/316L dissimilar welded samples, the average UTS was reduced from 476 MPa at ambient temperature up to 418 MPa at 300 ºC. At both ambient and elevated temperature, the 304L welded samples exhibited higher average UTS when compared with the 316L similar welded samples as well as the dissimilar 304L/316L welded samples (see Fig. 7a). For example, at 300 ºC, the 304L, 316L and 316L/304L welded specimens exhibited average UTS of 484 MPa, 412 MPa and 418 MPa, respectively.

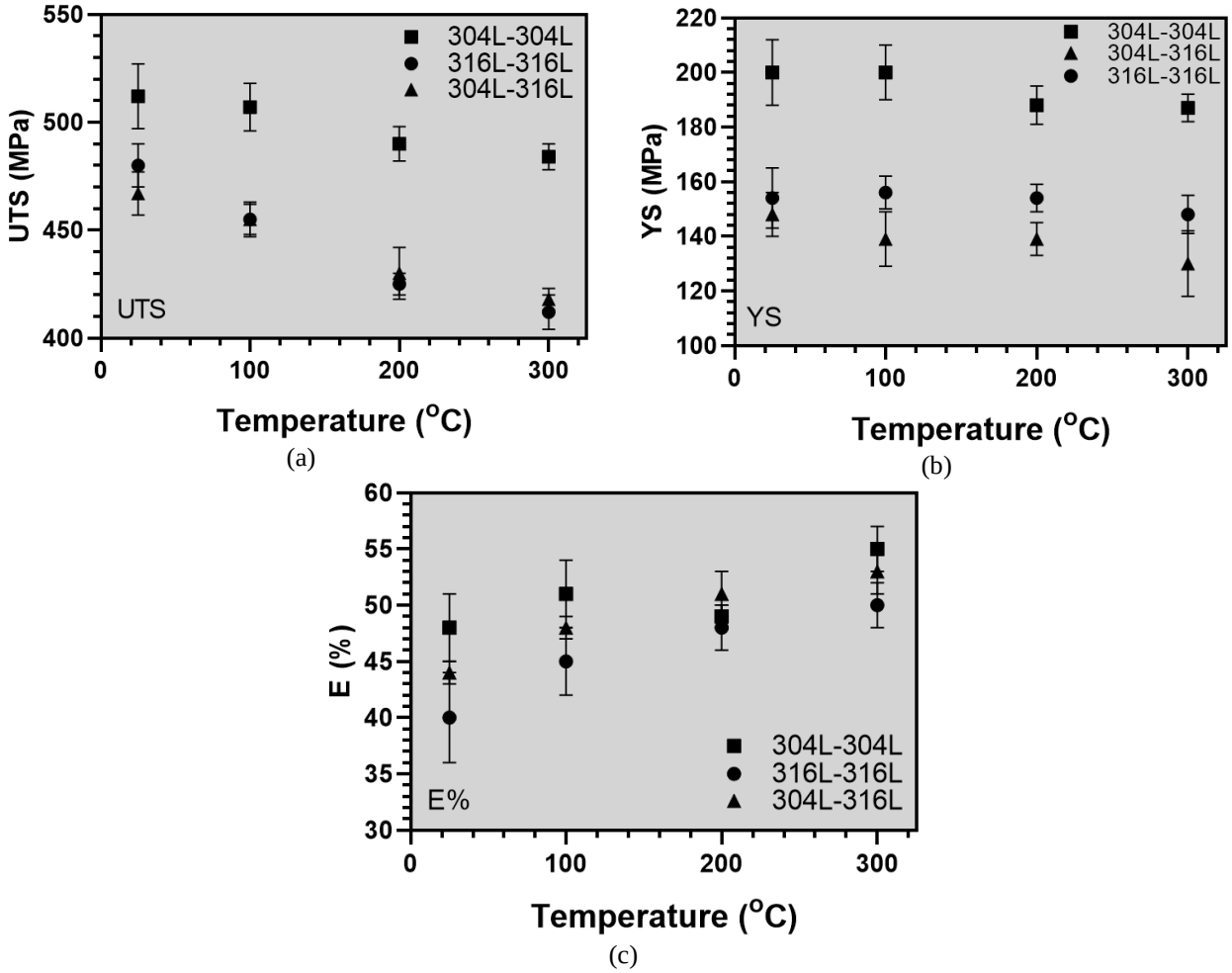

Figure 7. The variation of the UTS (a), YS (b) and %E (c) of the 304L, 316L and dissimilar 316L/304L ASSs weldments with the temperature.

Figure 7b shows the variation of the YS of the welded joints with temperature. At ambient temperature, the 304L similar weldments showed higher average YS (212±12 MPa) than the average YS of 304L base metal (200±8 MPa). Also, at ambient temperature, the 316L similar welded samples exhibited slightly lower average YS (165±11 MPa) than the 316L base metal (170±6 MPa). The dissimilar 304L/316L welded samples exhibited slightly lower average YS (156±8 MPa) than both 304L and 316L welded samples. Increasing the test temperature reduces the YS of the welded joints. Such observation was noticed for both similar and dissimilar 304L and 316L ASSs welded samples. For instance, increasing the test temperature of the 316L similar welded samples from ambient to 300 ºC, the average YS was reduced from 165 MPa to 155 MPa. While for 304L/316L dissimilar welded samples, the average YS was reduced from 156 MPa at ambient temperature up to 142 MPa at 300 ºC. Like the UTS, at both ambient and elevated temperature, the 304L welded samples exhibited higher average YS when compared with the 316L similar welded samples as well as the dissimilar 304L/316L welded samples.

Figure 7c shows the variation of the YS of the ASS welded joints with the temperature. At ambient temperature, the 304L similar welded samples showed higher average E% (48±5%) than the average E% of 304L base metal (45±3%). Also, at ambient temperature, the 316L similar welded samples exhibited slightly lower average E% (40±4%) when compared with 316L base metal (41±2 MPa). The dissimilar 304L/316L welded samples showed lower average E% (44±3 MPa) than the 304L similar joints, but, higher than the 316L welded samples. Increasing the test temperature increases slightly the E% of the welded joints. This observed for both similar and dissimilar 304L and 316L ASSs welded samples. For instance, increasing the test temperature of the 316L similar welded samples from ambient to 300 ºC, the average E% was increased from 40±4% to 50±2%. While for 304L/316L dissimilar welded samples, the average E% was increased from 44±3% at ambient temperature up to 53±2% at 300 ºC. Except at 200 ºC, the 304L welded samples showed higher average E% when compared with the 316L similar welded samples

International Journal of Engineering Research & Technology (IJERT)
ISSN: 2278-0181
Vol. 11 Issue 02, February-2022

as well as the dissimilar 304L/316L welded samples. At temperature of 200 ºC, the 304L/316L dissimilar welded specimens exhibited the highest E%, followed by the 304L similar welded sample.

3.4. ANN Modelling of the tensile characteristics of stainless-steel welded joints

The ANN modelling results revealed that the MLP and RBF ANN models with 2-5-3 and 2-9-3 structures, respectively, were found to have the best performances for modelling the tensile properties (UTS, YS and E%) of the welded joints. The RBF 2-9-3 ANN model exhibited 94.173%, 93.038 and 91.159% for the training, test, and validation performances, respectively. The MLP model exhibited 94.007%, 94.842 and 89.912% for the training, test, and validation performances, respectively. Figure 8 shows a comparison between the target and the output UTS, YS and E% values. For UTS, it has been found the MAE generated from the MLP and RBF models are about 6.788 and 6.472, respectively. For YS, the MAE generated from the MLP, and RBF models were about 6.21 and 6.55, respectively. While, for the E%, the MAE generated from the MLP, and RBF models were about 1.93 and 2.65, respectively.

The results revealed that the ANN models of the tensile properties of 304L and 316L similar and 304L/316L dissimilar ASS welded joints showed very good accuracy. The experimental and the predicted values of the tensile properties were close to each other. The MLP ANN modelling approach showed slightly better accuracy, when modelling the YS and E%, when compared with the RBF modelling approach. However, The RBF ANN modelling approach showed slightly better accuracy than the MLP approach when modelling the UTS.

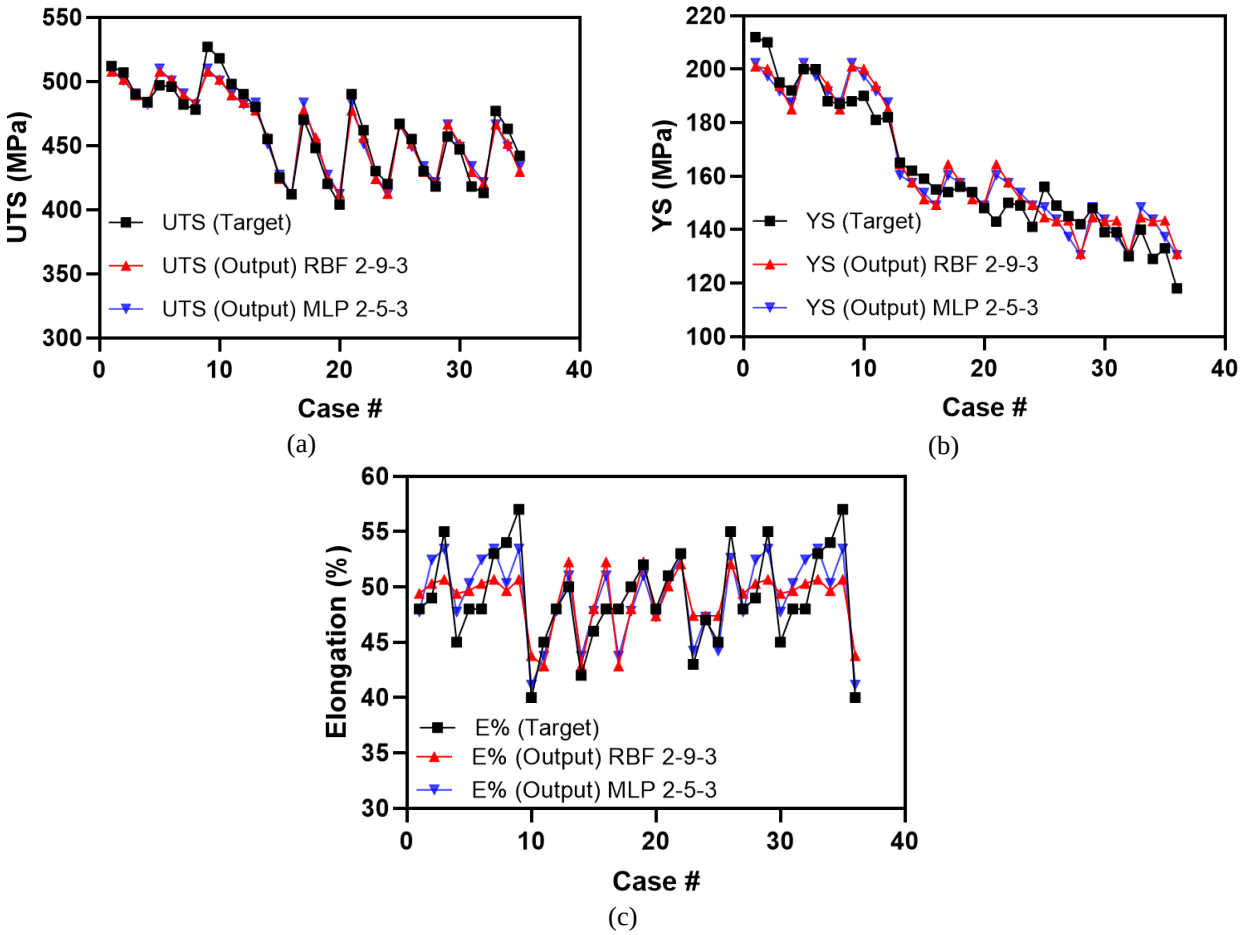

Figure 8. Comparison between the target and the output of (a) UTS, (b) YS and (c) E% values resulted from the ANN models.

4. CONCLUSIONS

1. The fusion zones, of the 304L and 316L similar and dissimilar welded regions, exhibited slightly higher hardness when compared with the base metals. The average hardness follows a decreasing trend in the order of weld metal, HAZ and BM. The center of the fusion zones of 304L, 316L and 316L/304L weld metals exhibited average hardness of 207+2 VHN, 207+3 VHN and 209+3 VHN, respectively.
2. Increasing the test temperature reduces the UTS and YS of the 304L and 316L similar and 316L/304L dissimilar weldments. However, increasing the test temperature was found to increase the ductility of the stainless-steel welded joints.
3. The models constructed based on MLP and RBF ANN techniques with of 2-5-3 and 2-9-3, layer structures, respectively, exhibited the best performances for modelling the tensile properties of the welded joints. The RBF 2-9-3 ANN model

International Journal of Engineering Research & Technology (IJERT)
ISSN: 2278-0181
Vol. 11 Issue 02, February-2022

showed training, test, and validation performances of 94.173%, 93.038 and 91.159%, respectively. While the MLP model exhibited about 94.007%, 94.842 and 89.912% for training, test, and validation performances, respectively. The mean relative error (MAE) generated from the MLP and RGB models were about 7.69 and 7.45, respectively.

4. The generated ANN models were successfully used to predict the tensile characteristics of 304L and 316L similar as well as the 316L/304L dissimilar ASS welded joints with an acceptable accuracy. The generated ANN models may be used to correlate the tensile properties of the welded joints with the temperature.

ACKNOWLEDGMENTS

The authors of the current investigation are grateful to Faculty of Engineering at Shoubra (Benha University) for providing the materials and welding machine and test equipment used in the current work.

REFERENCES

[1] John C. Lippold, Damian J. Kotecki, “Welding Metallurgy and Weldability of Stainless Steels”, 1st Edition, Wiley-Interscience, 2005.
[2] Pierre-Jean Cunat, “The Welding of Stainless Steels”, 2nd Edition, Euro Inox, Materials and Applications Series, Volume 3, 2007.
[3] Kondapalli Siva Prasad, Chalamalasetti Srinivasa Rao, and Damera Nageswara Rao, “A Review on Welding of AISI 304L Austenitic Stainless Steel”, J. Manuf. Sci. Prod., 2014, 14(1), pp. 1–11.
[4] C. Tembhurkar, R. Kataria, S. Ambade, J. Verma, A. Sharma and S. Sarkar, “Effect of fillers and autogenous welding on dissimilar welded 316L Austenitic and 430 ferritic stainless steels”, J. Mater. Eng. Perform., 2021, 30, pp. 1–10.
[5] Harsh Kukreja, N. Bharath, C. S. Siddesh, S. Kuldeep, “An Introduction to Artificial Neural Network”, International Journal of Advance Research and Innovative Ideas in Education, 2016, 1(5), pp. 27-30.
[6] D. T. Pham, M. S. Packianather, A. A. Afify, “Artificial Neural Networks”, D. Andina and D.T. Pham (eds.), Computational Intelligence, Chapter 3, Springer, 2007, pp. 67–92.
[7] R. Sudhakaran, V. VelMurugan, P.S. Sivasakthivel, M. Balaji, “Prediction and optimization of depth of penetration for stainless steel gas Tungsten arc welded plates using artificial neural networks and simulated annealing algorithm”, 2011, Neural Computing and Applications, 22(3-4), pp. 637-649.
[8] Laurent Jacques, Abderrazak El Ouafi, “ANN Based Predictive Modelling of Weld Shape and Dimensions in Laser Welding of Galvanized Steel in Butt Joint Configurations”, Journal of Minerals and Materials Characterization and Engineering, 2018, 6, pp. 316-332.
[9] Kamel Oussaid, Abderazak El Ouafi, “A Study on Prediction of Weld Geometry in Laser Overlap Welding of Low Carbon Galvanized Steel Using ANN-Based Models”, Journal of Software Engineering and Applications, 2019, 12, pp. 509-523.
[10] Tapas Bera and Santanu Das, “Application of Artificial Neural Networks in Predicting Output Parameters of Gas Metal Arc Welding of Dissimilar Steels’, Indian Science Cruiser, 2021, 35(3), pp. 26-30.
[11] H. Ates, B. Dursun and E. Kurt, “Estimation of mechanical properties of welded S355J2+N steel via the artificial neural network”, Scientia Iranica B, 2016, 23(2), pp. 609-617.
[12] American Society for Testing and Materials, ASTM E407-07, “Standard Practice for Micro-etching Metals and Alloys”, 2007.
[13] Sindo Kou, “Welding metallurgy”, John Wiley & Sons, 2003.
[14] Mohammad Shirdel, Hamed Mirzadeh, And Mohammad Habibi Parsa, “Microstructural Evolution During Normal/Abnormal Grain Growth in Austenitic Stainless Steel”, Metallurgical and Materials Transactions A, 2014, Vol. 45A, pp. 5185-5193.
[15] Wichan Chuaiphan, Loeshpahn Srijaroenpramong, “Evaluation of microstructure, mechanical properties and pitting corrosion in dissimilar of alternative low-cost stainless-steel grade 204Cu and 304 by GTA welding joint”, J. material res. Technol, 2020, 9(3), pp. 5174–5183.
[16] T.D. Anderson, M.J. Perricone, J.N. Dupont, A.R. Marder, “The influence of molybdenum on stainless steel weld microstructure”, Weld Res, 2007, 86, pp. 281-292.